VERTICAL LOAD TEST ON A DRILLED SHAFT INSTALLED IN GLACIALLY DERIVED SEDIMENTS

Ghada S. Ellithy, U.S. Army – Engineer Research and Development Center, Vicksburg, MS, USA, 601.634.7433, ghada.s.ellithy@usace.army.mil
Robert C. Simpson, Loadtest, Atlanta, GA, USA, 800.368.1138,
bob@loadtest.com

ABSTRACT

There are several methods for estimating the axial capacity of drilled shafts installed in coarse-grained soils. Most methods estimate the ultimate capacity for side friction and tip resistance. Design capacity is then calculated by applying a resistance factor to the ultimate capacity. In reality, however, ultimate resistance may not be mobilized except after a significant displacement that is not structurally tolerated in either compression or tension modes.

A full- scale load test is the best way to obtain the load settlement curve for a drilled shaft, especially in soil formations where accurate estimation of soil frictional properties from a field investigation may be difficult. This paper presents the results of a static, axial, compressive bi-directional load test, using the Osterberg method (O-cell test). The test was designed so that the shaft above the O-cell would move up and the shaft below it would move down when loaded. At the start of the test the concrete around the O-cell is fractured generally on a plane near the bottom of the cell.

The test was designed to validate the design capacity of drilled shafts embedded into the Vashon recessional outwash (Qvro), which is a glacially derived sediment consisting of thick deposits of cobbly sand and gravel relatively free of silt and clay found in the Seattle, WA area. The test shaft consisted of a 2.5- feet (0.75 m) diameter drilled shaft. The test shaft was installed to a depth of about 47 feet (14.3 m) into this formation. A maximum load of 437 kips (1.95 MN) was applied during the test, in each direction. The maximum load was attained at upward and downward displacements of less than 0.1 inch (2.5 mm), respectively.

Although the load test did not yield ultimate values, the results are compared to the design assumptions using methods adopted in the FHWA and AASHTO guidelines, which verified the adequacy of the design assumptions. We conclude that more emphasis is needed in the prediction of the service loads and corresponding mobilized displacement that may lead to a more cost effective design. It is also clear that more testing to higher loads could lead to more efficient designs on specific projects and generally as data is added to the local knowledge base.

Keywords: Drilled shafts, Osterberg method, bi-directional load test, glacial sediments, mobilized side friction, mobilized end bearing

INTRODUCTION

Drilled shafts have been widely used as a foundation system for high buildings and towers to support both axial and lateral loads especially in areas where seismic loading is present. Numerous research efforts have been conducted on drilled shafts installed in cohesionless soils consisting of sands and gravels under vertical loads; however, to the knowledge of the authors, there are few published results of load tests in glacially derived deposits. The vertical load test presented in this paper was performed on a drilled shaft embedded into the Vashon recessional outwash (Qvro), which is a glacially derived sediment consisting of thick deposits of cobbly sand and gravel relatively free of silt and clay present in the Seattle, WA area. A variety of load tests have been conducted in the Troutdale formation in and around Portland, Oregon. The

subsurface material, specifically the Troutdale, is very similar to the Ovro. In several cases, ultimate values were obtained.

To improve the design analysis methods for estimating vertical capacity of drilled shafts in these glacial derived deposits, there is a need for additional high quality vertical load test data. The main objectives of this paper are twofold: (1) to present the results of a vertical load test on a fully instrumented 29.5-inch-diameter drilled shaft embedded in glacial derived deposits, and (2) to validate the design assumptions based on existing FHWA and LRFD criterion (O'Neil and Reese 1999) using the compiled vertical load test data presented in this paper.

TEST SITE CONDITIONS

The U.S. Army Corps of Engineers, Seattle District supervised the design and construction of the air traffic control tower (ATCT) in Lakewood, WA (about 40 miles south of Seattle) and its deep foundation system consisting of a pile cap supported on eighteen uncased 47-foot- long drilled shafts. During the design stage, a decision was made to perform a testing program to ensure the adequacy of the design as far as the drilled shaft compression and tension capacity and to gather information for future design in the same subsurface conditions that have few documented field tests. The load test was conducted on a sacrificial test drilled shaft that was constructed in the middle of the ATCT footprint.

The soil borings drilled in the vicinity of the ATCT encountered layers of sands and gravels extended from the ground surface to about 70-feet deep. The upper layers consisted of top soil and man-made fill material that extended to about elevation 300 which is the bottom of the pile cap at 10 feet below the ground surface. Below this elevation, the soil layers consisted of the Vashon recessional outwash (Qvro) deposits that were left by outburst floods and meltwater streams flowing from the margin of the Vashon ice sheet as it wasted and retreated from the Puget Lowland. Qvro deposits in the project area compose the majority of soils encountered.

Qvro typically consists of loose to very dense, poorly graded and well-graded, sandy gravel, sand, and gravelly sand with variable amounts of silt, clay, cobbles, and boulders. Qvro is locally interbedded with fine-grained layers. These layers may be overbank deposits or deposits that accumulated in quiet water depressions within the outwash plain. The soils encountered in the borings generally varied in their relative density from loose to very dense and generally increased with depth; however, loose sands were encountered at lower depths.

CONSTRUCTION OF THE TEST SHAFT AND INSTRUMENTATION

The nominal 29.5-inch- diameter test shaft was excavated dry to a base elevation of about +252.7 feet in the middle of the pile cap footprint. The shaft was drilled by installing a 29.5-inch outer diameter (OD) segmented casing using a rig-mounted rotary tool as the drilling progressed. An auger was used for drilling the shaft, and a clean-out bucket for cleaning the base. After the shaft was approved for concrete placement, the carrying frame with attached bi-directional loading assembly and instrumentation was inserted into the excavation and temporarily supported from the drilling rig. Concrete was then delivered by pump through a 5-inch OD pipe into the base of the shaft until the top of the concrete reached an elevation of 300 ft. The contractor removed the 29.5-inch OD casing in sections as the concreting progressed. The specified concrete strength was 4000 psi, construction of the test shaft was completed on December 03, 2015 and the test was performed on December 11, 2015 where temperature was 46^{o}F on average, cloudy skies and no precipitation. Fig. 1 shows photos during the construction of the test shaft.

The loading assembly consisted of a single 9-inch- diameter O-cell, located 11.0 feet above the shaft base. It was calibrated to 538 kips and then welded closed prior to shipping. Embedded testing instrumentation included the following:

- Paired upper compression telltale casings (nominal ½-inch steel pipe) attached diametrically opposed to the carrying frame, extending from the top of the loading plane to ground level.
- Four Linear Vibrating Wire Displacement Transducers (LVWDTs)) positioned between the lower and upper plates of the loading plane.
- One level of two sister bar vibrating wire strain gages (VWSGs) attached diametrically opposed to the carrying frame below the base of the loading plane. Two levels of two VWSGs attached diametrically opposed to the carrying frame above the top of the loading plane.
- Two lengths of ½-inch steel pipe, extending from the top of the shaft to the top of the bottom plate, to vent the break in the shaft formed by the expansion of the O-cell and to accommodate bottom plate telltales. Fig. 2 shows details of the instrumentation placement and strain gage positions.

Fig. 1 Installation of the loading assembly and concreting the drilled shaft

TEST SET-UP AND PROCEDURES

Test Arrangement

Throughout the load test, key elements of shaft displacement response were monitored using the equipment and instruments detailed below: Top of shaft displacement was monitored using a pair of automated digital survey levels. Upward displacement was measured using ¼-inch telltale rods positioned inside casings and monitored by vibrating wire displacement transducers.

- Downward displacement was measured using ¼-inch telltale rods positioned inside casings and monitored by vibrating wire displacement transducers attached to the top of the shaft.
- Expansion of the loading assembly was measured using four embedded vibrating wire displacement transducers.
- A bourdon pressure gage, vibrating wire pressure transducer and a voltage pressure transducer were used to measure the pressure applied to the O-cell at each load interval.

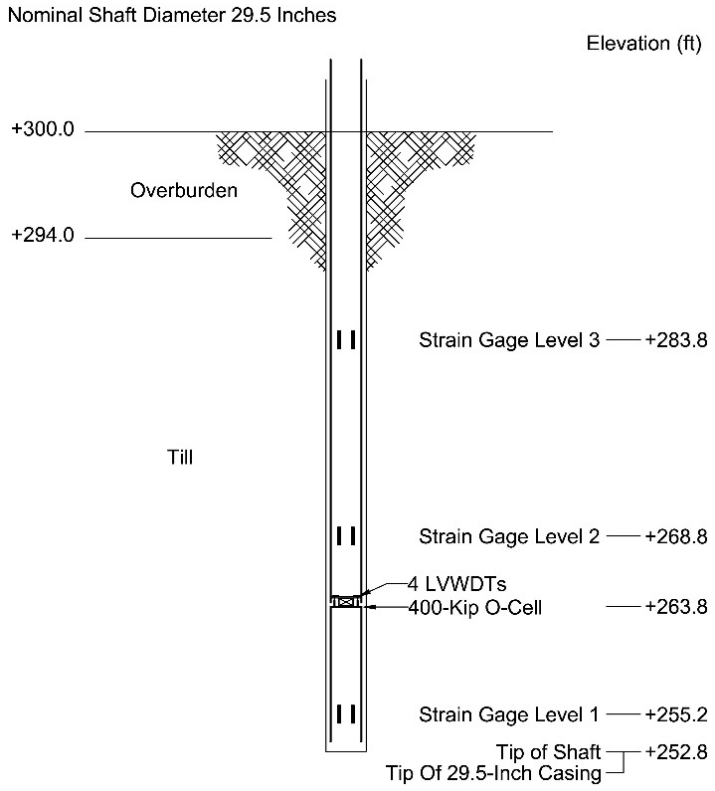

Fig. 2 As- built schematic section of the test shaft

Data Acquisition
All instrumentation were connected through an electronic data logger connected in turn to a laptop computer.

Testing Procedures
Testing was begun by pressurizing the O-cell in order to break the tack welds that hold it closed (for handling and for placement in the shaft) and to form the fracture plane in the concrete surrounding the its base. After the break occurred, the pressure was immediately released and the testing recommenced from zero pressure.

The load increments were applied using the Quick Load Test Method for Individual Piles, ASTM D1143/D1143M – 07 (2013). Each successive load increment was held constant for eight minutes by automatically adjusting the applied pressure. Approximately one minute was used to move between increments. The O-cell was pressurized in 15 nominally equal increments, resulting in a maximum bi-directional load of 437 kips applied to the shaft above and below the loading plane. The loading was halted after increment 1L-15 because the maximum capacity of the loading apparatus had been exceeded. The shaft was then unloaded in five decrements, and the test was concluded.

LOAD TEST RESULTS

General
The loads applied during a bi-directional test act in two opposing directions, counteracted by the resistance of the shaft above and below. It is assumed that no additional upward load is applied until the expansion force exceeds the buoyant weight of the shaft above the loading assembly. Therefore, *net load*, which is defined as gross applied load minus the buoyant weight of the shaft above the loading assembly, is used to determine side shear resistance above it and to construct the equivalent top load displacement curve. For this test, a shaft buoyant weight of 25 kips was calculated.

Upper side shear resistance
The loading assembly applied a maximum upward *net load* of 412 kips to the upper side shear at load interval 1L-15. At this loading, the upward displacement of the top of the O-cell was 0.090 inches (Fig. 3).

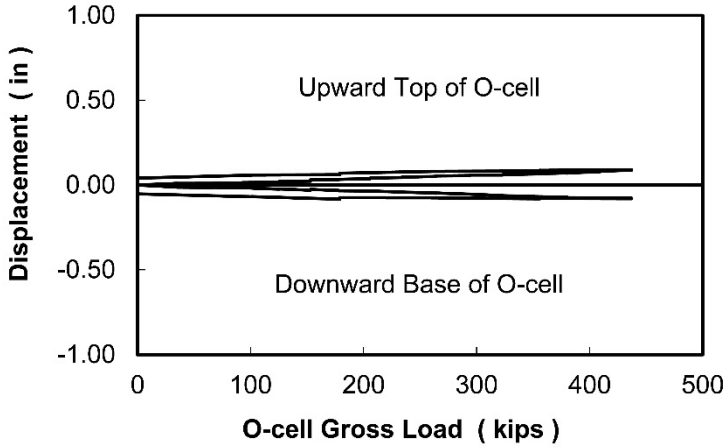

Fig. 3 Load vs. displacement plot

Combined end bearing and lower side shear resistance
The loading assembly applied a maximum downward load of 437 kips at last load interval. At this loading, the average downward displacement was 0.080 inches (Fig 3). The load resisted by side shear in the 2.5-foot shaft section below the Level 1 strain gages is subtracted to determine the maximum applied end bearing load of 101 kips. The unit end bearing at the base of the shaft is calculated to be 21.2 ksf (Fig. 4).
Strain gage analysis
Using the ACI formula ($E_c=0.033 \times \gamma_c^{1.5} \times \sqrt{f'_c}$) , the area of reinforcing steel and nominal shaft diameter, provided an average shaft stiffness (AE) of 3,050,000 kips along the length of the shaft. The stiffness allows loads to be calculated at the various strain gage elevations. The load distribution curves for each load increment, based on the applied load and computed strain gage loads, are presented in Fig. 5. T-Z curves are presented in Fig. 6.

Equivalent top load-displacement
Fig. 7 presents the equivalent compression top load (ECTL) curve. The curve is generated by Loadtest (2007), assuming the load is applied at the top of shaft (+300.0 ft.). A combined side shear and end-bearing resistance of 849 kips was mobilized during the test. The plotted ECTL curve includes the additional elastic compression of a top-loaded shaft.

Equivalent tension top load-displacement

Fig. 7 also presents the equivalent tension top load (ETTL) curve. The curve is generated by Loadtest (2007), assuming the load is applied at top of shaft (+300.0 ft.) but also assuming that the end bearing resistance is zero. The plotted ETTL curve includes the additional elastic compression of a tension top-loaded shaft.

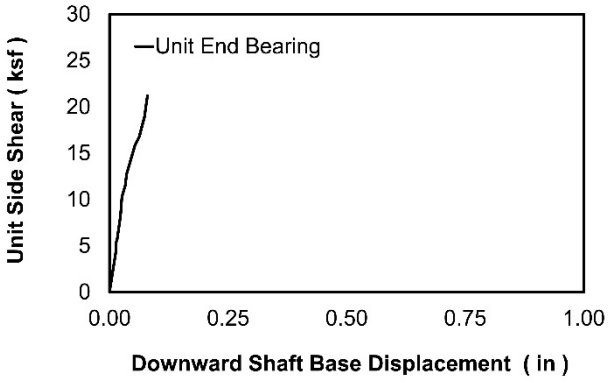

Fig. 4 Mobilized unit end bearing

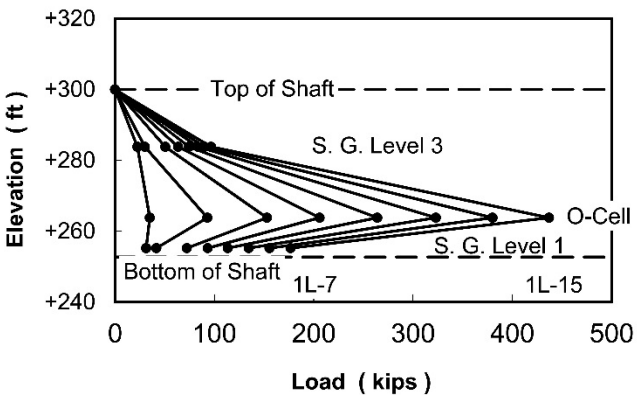

Fig. 5 Strain Gage load distribution

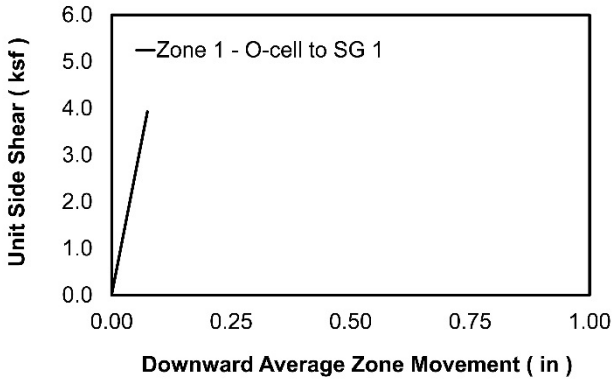

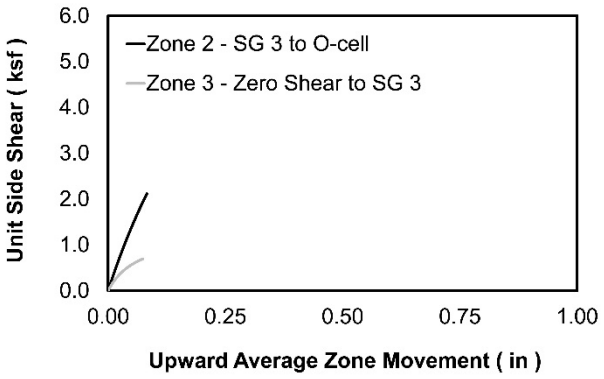

Fig. 6 a) Mobilized downward net unit side shear, b) Mobilized upward net unit side shear

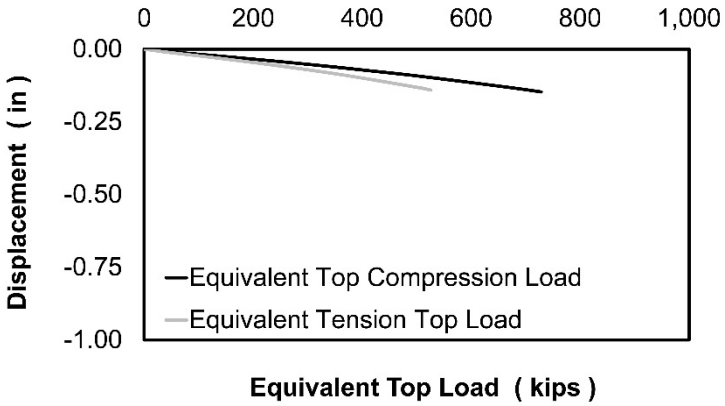

Fig. 7 Equivalent top load-displacement

DESIGN ASSUMPTIONS

During design, the axial resistance of the drilled shafts was evaluated in accordance with the USACE EM 1110-1-1905 and FHWA IF-99-025 adopting limit state design approach per AASHTO (2010), which allows for performance factors to be applied to different resistance components; side friction and base resistance. The Allowable Strength Design (ASD) method as specified in the IBC code could be used as well by considering the factored strength limit resistance to be the value to be used for allowable design capacity including side and tip resistances.

Axial resistance analyses were performed originally for cast-in-place, uncased reinforced concrete 24-inch-diameter drilled shafts based on side friction resistance and base resistance for service settlement limits of 0.5 and 1.0 inch, and for strength limit based on ultimate side friction resistance and ultimate base resistance. It was decided that the drilled shaft base be founded at least 5 feet below the dense to very dense sandy gravel layer at or below elevation 270 feet. For design, some conservative assumptions were made to account for variability of the subsurface conditions and the possibility of presence of loose sand seams, also considered a shallow potential water table at about elevations 282 feet.

Due to construction constraints related to drilling temp casings in gravelly material with cobbles, the built-in diameter of the drilled shafts was changed to 29.5 inch, and a decision was made not to change the embedment depth into the Qvro deposits. Different approaches for drilled shafts resistance are based on empirical factors derived from in-situ test. While many field load tests have been performed on drilled shafts in clays, fewer have been performed on drilled shafts in sands and gravels which initiated this study to compare field load test results with the design assumptions.

Side Resistance

The FHWA design method, O'Neill and Reese (1999), assumes that the drilled shaft resistance in cohesionless soils is independent of the soil friction angle or the *SPT* blow count where the friction angle approaches a common value due to high shearing strains in the sand caused by stress relief during drilling. The method uses a load transfer coefficient β. The nominal axial unit side resistance, q_s in ksf is calculated using the β-method as follows:

$$q_s = \beta\sigma_v' \qquad \text{Eq. 1}$$

where σ_v' is the vertical effective stress at soil layer mid-depth in ksf and is a dimensionless load transfer coefficient. For $N_{60} \geq 15$, $\beta = 1.5–0.135\ (z)^{0.5}$ in sands, and $\beta = 2.0 – 0.06(z)^{0.75}$ in gravels, where; z is the depth below ground at soil layer mid-depth in feet, and N_{60} is the corrected (for hammer efficiency only) average SPT blow count in the design zone in blows/ft. For $N_{60} < 15$, $\beta = N_{60} * (1.5\text{-}0.135(z)^{0.5}/15$ in sands and gravels. β has a min value of of 0.25 and a max value of 1.2 in sands and 1.8 in gravels. The O'Neill and Reese (1999) method recommends q_s be limited to 4 ksf. The above design calculations were used for both compressive and tension capacity estimates; however, AASHTO LRFD (2010) recommends a lower resistance factor that results in tension capacity of about 0.8 of the side friction portion of the compressive capacity.

Tip Resistance

Using the FHWA design method, the nominal unit tip resistance, q_p. in ksf is calculated using Eq. 2:

$$q_p = 1.2N_{60} \qquad \text{Eq. 2}$$

The O'Neill and Reese (1999) method recommends q_p be limited to 60 ksf unless greater values can be justified through load test data. If SPT-N60 blow counts are greater than 50, but limited to 100, which was the case in Qvro layers at the base / tip of the drilled shaft, tip resistance in ksf can be calculated using Eq.3:

$$q_p = 0.59\left[N_{60}\left(\frac{P_a}{\sigma_v'}\right)\right]^{0.8}\sigma_v' \qquad \text{Eq. 3}$$

where P_a is atmospheric pressure = 2.12 ksf. Eq 3. Was checked for calculating the unit tip resistance, however, the difference was not significant and the value was estimated at 60 ksf.

Settlement

Figs. 8.a and 8.b show the normalized load-displacement curves in side resistance and in end bearing, respectively, in cohesionless soils. Fig. 8 was used to compute the drilled shaft resistance for service limit

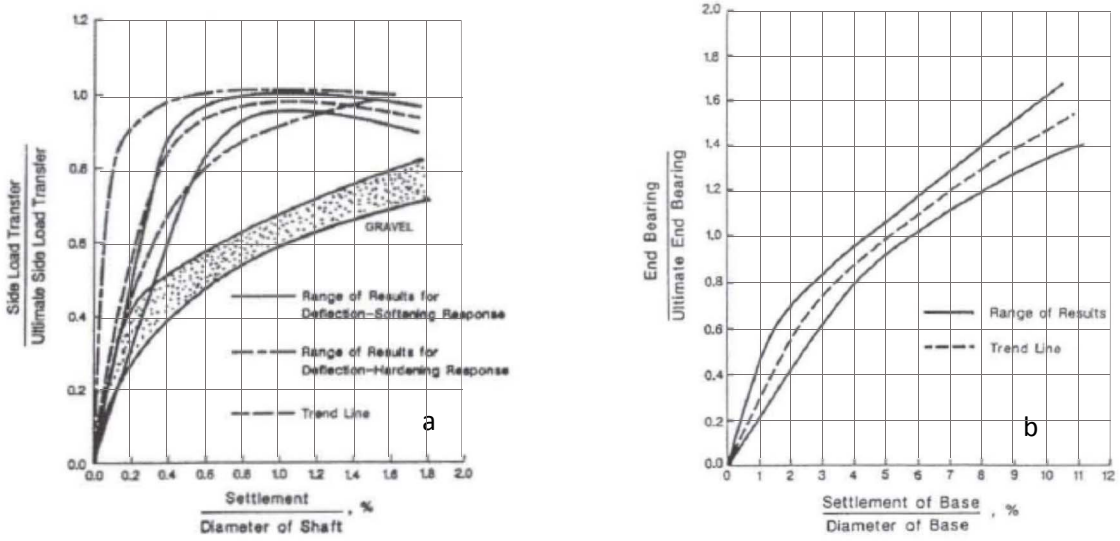

Fig. 8 Normalized load transfer versus settlement in cohesionless soils; a) side resistance, b) end bearing (from O'Neill and Reese, 1999)

state movement values of 0.5 and 1.0 inch using trend curves. Fig. 8.a shows that the skin friction is typically fully mobilized at displacements of 0.2% to 1% of the shaft diameter depending on the nature of deflection response and whether it is a deflection-softening or deflection-hardening. Fig. 8.b shows that settlement due to end bearing loading often does not exhibit a break point or well defined failure, and that end bearing resistance continues to increase as the settlement increases beyond 5% of the base diameter which is typical when end bearing is fully mobilized for drilled shafts in cohesive soils.

COMPARISON BETWEEN LOAD TEST RESULTS AND DESIGN VALUES

The curves in Fig. 8 were used for the purpose of validating design assumptions with load test results. The drilled shaft axial capacity was recalculated for a 29.5- inch- diameter size and presented as plots with depth of mobilized resistance at 0.1- inch settlement using the upper, lower, and trend curves. The ultimate resistance was also added for comparison as shown in Fig. 9.

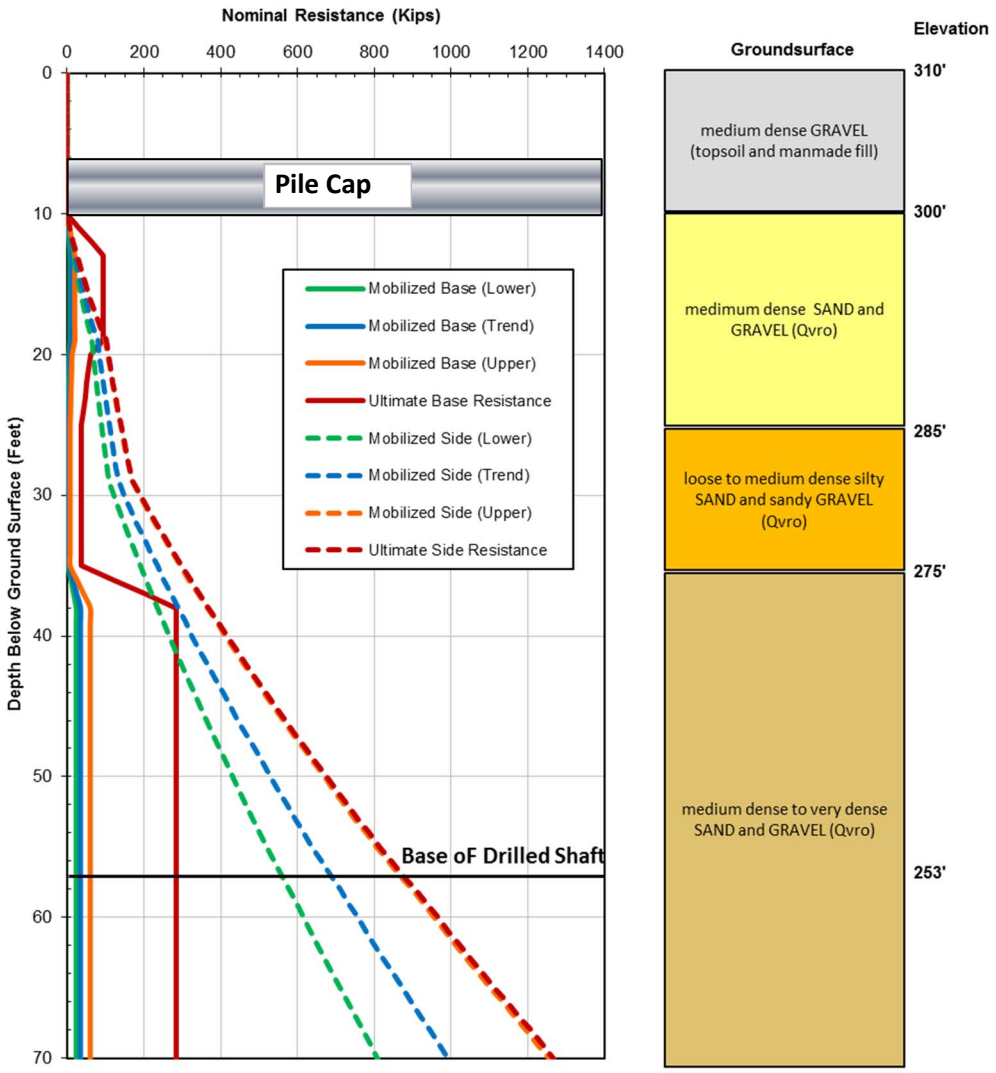

Fig. 9 Estimated ultimate and mobilized axial resistance at 0.1 inch of 29.5 inch diameter drilled shaft

Due to a late construction decision to increase the shaft diameter to 29.5 inch from the proposed design size of 24 inch, the shaft capacity increased but the test capacity did not. Partly as a result of this and as a result of greater than expected resistances, the ultimate capacity of the shaft could not be reached.

Fig. 7 shows that about 550 kips were mobilized as an equivalent top compressive load at a settlement of 0.1 inch or 0.34% normalized settlement. This value matches the lower mobilized side friction for the embedded shaft length per the FHWA method as shown in Fig. 9. Other point values on the load-displacement curve suggest that the Qvro exhibits a deflection-hardening response. At about 0.5% of normalized settlement, the mobilized unit side friction reaches a value of 3.9 ksf (Fig. 6.a) close to the max allowed of 4 ksf. This suggests that for such deposits, a max unit side friction could be increased by about 20% and a value of 5 ksf could be used. Fig. 7 shows about 400 kips were mobilized as an equivalent top tension load at a settlement of 0.1 inch. This value compared to corresponding compressive load mobilized at the same displacement is about 70%, which may suggest that resistance factor for tension loads in such deposits should be lowered to 70% instead of 80% of the compressive loads.

Fig. 4 shows a mobilized unit end bearing of about 21 ksf or 0.35 normalized end bearing capacity at a displacement of less than 0.1 inch. This value corresponds to a mobilized end bearing load of about 100 kips, which is higher than the upper bound shown on Fig. 9 of about 60 kips. This result suggests that the upper bound curve of mobilized end bearing should be steeper at lower displacements allowing for higher mobilized end bearing. Load testing in similar deposits need to be conducted at higher loads to examine the mobilized end bearing at 5% normalized displacement and compare the corresponding unit end bearing to the currently accepted 60 ksf.

SUMMARY AND CONCLUSIONS

The results of the bi-directional, static, compressive, axial load test were presented. A comparison was made between the unit end bearing pressure and unit side friction used in the design and the ones calculated from the load testing for Vashon recessional outwash layers (Qvro). The data presented in this paper show that the mobilized side friction at the site for the Qvro exhibited a deflection-hardening response and that ultimate unit skin friction could be increased to 5 ksf. Measured equivalent top load in tension suggests that resistance factors for tension loads in similar deposits should be in the range of 70% instead of 80% of the compressive loads. The mobilized end bearing exceeded the assumed values based on the FHWA design method by about 65%, which allows for increasing the ultimate design values taking into consideration the serviceability requirements of the structure. Ultimate end bearing mobilized at 5% normalized displacement needs to be further examined by a higher capacity load testing.

REFERENCES

American Association of State Highway and Transportation Officials (AASHTO). 2010. LRFD Bridge Design Specifications.

American Society for Testing and Materials (ASTM). 2013. Standard Test Methods for Deep Foundations Under Static Axial Compressive Load D1143/D1143M-07.

Loadtest USA. 2007. Construction of the Equivalent Top Load-Displacement Curve, Appendix C.

O'Neill, M.W., and Reese, L.C. 1999. Drilled Shafts: Construction Procedures and Design Methods. Publication No. FHWA-IF-99-025, Federal Highway Administration, Washington, D.C.

U.S. Army Corps of Engineers. 1992. Bearing Capacity of Soils, Engineering Manual EM 1110-1-1905.